Romanian Reports in Physics **71**, 207 (2019)

ANGULAR AND SPATIAL DISTRIBUTIONS OF PROTONS CHANNELED IN A BENT AND RADIALLY DEFORMED SINGLE-WALL BORON-NITRIDE NANOTUBES

D. BORKA[1,a], S. M. D. GALIJAŠ[2]

[1]Atomic Physics Laboratory (040), Vinča Institute of Nuclear Sciences,
University of Belgrade, P. O. Box 522, 11001 Belgrade, Serbia
Email:[a] *dusborka@vin.bg.ac.rs*
[2]Faculty of Physics, University of Belgrade, P.O. Box 368, 11001 Belgrade, Serbia
Email: *galijas@ff.bg.ac.rs*

Received April 23, 2018

Abstract. This study is devoted to the angular and spatial distribution of protons channeling through a bent and radially deformed single-wall boron-nitride nanotubes (SWBNNTs). These nanotubes are more thermal and chemical stable then carbon nanotubes, and they are good candidates for future channeling experiments. This investigation is continuation of our previous study [1, 2] and now we investigate channeling properties of SWBNNTs as a function of the very realistic effects: bending angle of nanotube and its radial deformation. For the first time we presented here investigation of these effects with boron-nitride nanotubes and combination of both effect. The angular and spatial distributions of channeled protons were generated using the Molière's expression for the continuum potential of the SWBNNT's atoms and computer simulation method. We also calculate the total yield of protons channeled in the nanotubes as a function of the bending angle. We demonstrate that varying bending angle and taking into account radial deformation we can get a significant rearrangement of the propagating protons within the boron-nitride nanotube. This investigation may be very useful to give us detailed information on the relevant interaction potentials inside SWBNNTs and for creating nanosized proton beams to be used in different applications in medicine and materials science.

Key words: Nanotubes, radial deformation, channeling, spatial and angular distributions.

1. INTRODUCTION

Noticing the similarities and differences between the already discovered carbon nanotubes (CNTs) [3] and boron nitride materials, Rubio *et al.* were theoretically predicted in 1994 [4] the stable boron nitride nanotubes using a very simple Slater-Koster tight-binding scheme. Immediately in the next year, the experimental confirmation of the existence of the boron nitride nanotubes (BNNTs) were made by Chopra *et al.* [5]. Due to the wide use of BNNTs nanotubes, numerous methods of synthesis have been developed such as arc discharge [6–8], chemical vapor deposition [9], substitution reaction [10, 11], ball milling [12–14], laser ablation

[15, 16] and low temperature methods [17], efficient for mass production of this kind of nanotubes. The structure of the BNNTs resembles the typical CNTs with carbon atoms substituted by nitrogen and boron atoms. Nevertheless, despite this similarity in structure, it is important to point out that almost all the physical and chemical properties of BNNTs are drastically different in comparison with CNTs [18–20]. Considering the thermal properties of SWBNNTs, a significant difference was found compared to CNTs. BNNTs have not only a greater specific heat [21] but also the high resistence to oxidation. Zhi and co-workers [22] established stability of the BNNTs at 1,100°C in air while the oxidation temperature for CNTs is approximately 500°C under the same condition, which means that boron nitride structure is chemically very stable [23].

In this work, investigation of 10 MeV proton beams guiding by the bent and radially deformed SWBNNTs is carried out. We point out, that the previous theoretical [24–30] considerations are related to the channeling of charged particles by carbon nanotubes. The first experimental channeling of the 2 MeV He^+ ions, also through multi-wall carbon nanotubes, was achieved by Zhu *et al.* [31]. Soon thereafter came another experimental confirmation. Chai *et al.* [32] successfully transmit the 300 keV electronic beam through the same nanotubes but in a different environment. Numerous simulations and theoretical investigations [33–49] get a detailed theoretical explanations of ion channeling processes by CNT's. In this paper, for the first time we take into account the radial deformation of the nanotubes together with the effect of nanotube bending.

2. THEORY

We consider a projectile proton launched with an initial energy of 10 MeV directed either along a line parallel to the axis or at some angle φ to the axis of the SWBNNT. The motion of the projectile and interaction between projectile and SWBNNT have been treated classically [50]. We chose the length of (10,10) SWBNNTs of order of μm to have the target that could be made using the existing techniques. After that, we chose the ion species and energy (protons of 10 MeV) to have the projectiles that can be delivered routinely using the existing accelerators. Also, these choice of ion species and energy is the same like in our previous work with (10,10) SWBNNTs [1], and this investigation is continuation of that work. In case of much higher proton energies (GeV) we have to use relativistic equations of motion [2]. For GeV protons, since the proton motion in the transverse plane is nonrelativistic, the corresponding equations of motion are made relativistically correct by using the relativistic proton mass instead of its rest mass. For keV energies protons it should be taken into account strong dynamic polarization of valence electrons

in the nanotubes which in turn will give rise to a strong image force on the protons, as well as a considerable energy loss due to the collective, or plasma, electron excitations [41]. For low energy proton channeling (eV energy region) we cannot neglect the electron capture from the nanotube wall by channeling proton, and this process will cause charging of the BN nanotube wall, like in case of insulating nanocapillary [51].

Our research of the angular and spatial distributions and channeling protons with the (10,10) SWBNNTs will be limited to the nanotubes that are not too long, since in this case the proton energy loss is negligible, but also long enough that the SWBNNT's ends do not affect a significant impact on the potential of the proton-nanotube interaction [1]. Finally, we do not take into account electron capture processes, because it's practically imperceptible [44].

In order to describe the channeling of protons through the SWBNNTs, we start with the right Cartesian coordinate system. It's convenient to set up the origin of the frame together with x and y axes at the entrance plane of the nanotube ($\rho^2 = x^2 + y^2$), which is normal in relation to the axis of the nanotube. Proton velocity is in direction of $-z$ axis. By $R = a_{BN} 10\sqrt{3}/2\pi$, we indicated the radius of the (10,10) SWBNNT without any kind of deformation, while the B-N bond lenght is denoted with a_{BN}. B-N bond lengths in B-N nanotubes is around 1.43 [52] or 1.44 Å [53]. We take values a_{B-N} = 1.44 Å. Distance d between B atoms in the B type atomic strings (the same distance is between N atoms in N type atomic strings) is $d = \sqrt{3} a_{B-N}$ = 2.49 Å = 0.249 nm. The total potential is the sum of potentials of 20 B type and 20 N type atomic strings (see Fig. 1 from the manuscript [1]).

For choice of parameters (the length of (10,10) SWBNNTs of 1 μm and 2 μm and projectile protons of 10 MeV) majority of protons make before leaving nanotube between one quarter of an oscillation and a few oscillations around the channel axis. For longer nanotubes we can not neglect the proton energy loss and the uncertainty of the proton scattering angle caused by its collisions with the nanotube electrons [29]. On the other hand (10,10) SWBNNTs consist of 40 straight atomic strings parallel to its axis, 20 atomic strings of B atoms (B type strings) and 20 atomics strings of N atoms (N type strings). If the length of the SWBNNTs is 1 μm and the distance d is 0.249 nm, it means that 1 μm long string contains arrays of around 4000 atoms. Thats why the effect of SWBNNT ends can be omitted.

Under external electric field or under external mechanical stress, SWBNNTs can have different geometrical shapes of the cross-section [54]. Let the x axis be oriented along the line that passes between the boron and nitrogen atoms. Due to radial deformation, the atoms of boron and nitrogen will be distributed along the ellipse in the transverse plane with $R_x = R(1-\eta)^{-1}$ and $R_y = R(1-\eta)$ as semi-major and semi-minor axes, respectively, where the parameter η determines the degree of radial deformation. For larger parameter values ($\eta > 0.35$), *i.e.* in the case of enormous

radial deformations, the shape of the ellipse is lost and will not be considered in this work [54]. In the plane perpendicular to the nanotube axis, the position of the boron and nitrogen atoms are given by the angle θ_k which is viewed in relation to the semi-major axis as

$$\theta_{kB} = \arctan\left(\frac{R_y}{R_x}\tan\left(\frac{2\pi(k-1)}{N} + \frac{\theta_{BN}}{2}\right)\right) \tag{1}$$

and

$$\theta_{kN} = \arctan\left(\frac{R_y}{R_x}\tan\left(\frac{2\pi(k-1)}{N} - \frac{\theta_{BN}}{2}\right)\right), \tag{2}$$

respectively, and by remoteness from the center of the SWBNNT R_k as

$$R_{kB(N)} = \frac{1}{\sqrt{\frac{1}{R_x^2} - \sin^2\theta_{kB(N)}\left(\frac{1}{R_x^2} - \frac{1}{R_y^2}\right)}}. \tag{3}$$

We can construct interaction potential between the proton and radially deformed bent SWBNNT using Molière's approximation of the Thomas-Fermi interaction potential [55] in the following form [27, 56]: $U(\rho) = \tilde{U}(\rho) + \frac{mv_0^2 x\alpha}{L}$, where the first term represent the proton-straight SWBNNT interaction potential given as

$$\tilde{U}(\rho) = \sum_{i=1}^{2}\frac{4Z_pZ_ie^2}{d}\sum_{k=1}^{N}\sum_{j=1}^{3}a_jK_0\left[b_{ij}\left[\left(R_{ik} - \rho\cos\theta_{ik}\right)^2 + \rho^2\sin^2\theta_{ik}\right]^{\frac{1}{2}}\right], \tag{4}$$

while the second term appears as a result of bending of the SWBNNTs. K_0 is the modified Bessel function of the second kind and zeroth order. The bending of the nanotube is along the positive direction of the x axis. We denote the bending angle by α and v_0 is the initial tangential velocity of the proton. The number of boron and nitrogen atomic strings which is the same for (10,10) SWBNNT we indicate with N (N = 20) while $(a_1, a_2, a_3) = (0.35, 0.55, 0.1)$, $(b_{i1}, b_{i2}, b_{i3}) = (0.3a_{tfi}^{-1}, 1.2a_{tfi}^{-1}, 6a_{tfi}^{-1})$, where the screening Thomas-Fermi radius a_{tfi} is functionally connected to the Bohr radius a_0 as $a_{tfi} = a_0(9\pi^2/128Z_i)^{1/3}$ and Z_p, Z_1 and Z_2 are the proton number of the proton, boron and nitrogen atoms, respectively. The average distance between two consecutive boron atoms or between two nitrogen atoms along their strings is $d = \sqrt{3}a_{BN}$ and e is the elementary charge value.

3. RESULTS AND DISCUSSION

We are investigated the influence of bending angle, radial deformation, nanotube lengths and protons energy on the angular and spatial distributions. The view along axis of a short straight not radially deformed SWBNNT (10,10) is given in

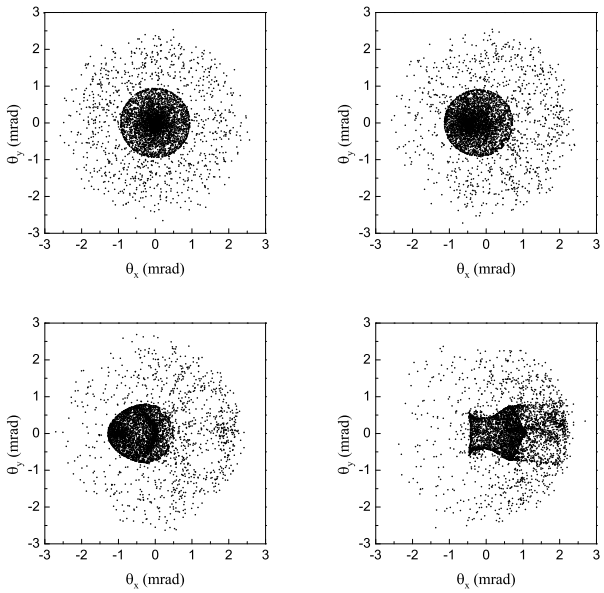

Fig. 1 – The angular distributions of protons channeled in the (10,10) SWBNNT in the $\Theta_x\Theta_y$ plane. The proton energy is E = 10 MeV, the nanotube length is $L = 1\mu$m and bent angle of the nanotube are: (left up) α = 0, (right up) 0.5 mrad, (left down) 1.0 mrad and (right down) 2.0 mrad.

Fig.1 in our previous paper [1]. In this study, we first analyzed influence of the nanotube bending angle on the angular and spatial distributions. Figure 1 shows the angular distributions of protons channeled in the (10, 10) SWBNNTs in the $\Theta_x\Theta_y$ plane whereas Fig. 2 shows the corresponding spatial distribution in the xy plane. The proton energy is E = 10 MeV and the nanotube length is L = 1 μm. The nanotube bent angle are analyzed in 4 cases: α = 0, 0.5, 1.0 and 2.0 mrad, respectively. We can notice that in both figures maximum yield of channeled protons is moved from the center of angular and spatial distributions. With increasing of bent angle this effect becomes stronger.

In Fig. 3 the spatial distributions along the x axis of protons channeled in the (10,10) SWBNNT with 4 different nanotube bent angles α = 0, 0.5, 1.0 and 2 mrad are presented. The proton energy is E = 10 MeV and the nanotube length is $L = 1\,\mu$m. We can see how variation of bending angles can move peak of yield within the nanotube. These effect can be used to manipulate with very narrow proton beams. This examination may be very useful to give us detailed information on the relevant interaction potentials inside SWBNNTs and for creating nanosized proton beams.

In Figs. 4 (left) and 4 (right) we presented the normalized yield of transmitted protons in bent nanotube and in case of donut effect and we compare these two

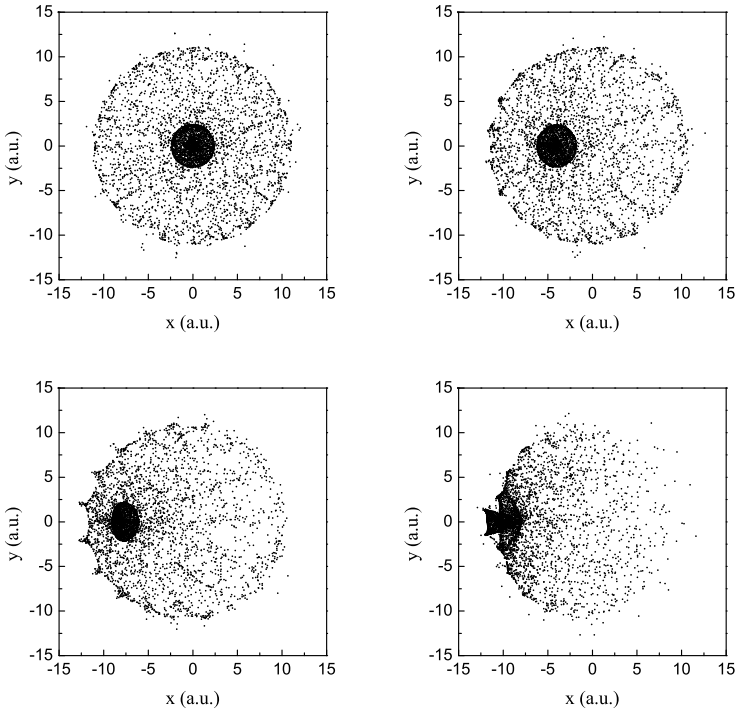

Fig. 2 – The same like Fig. 1, but for spatial distributions.

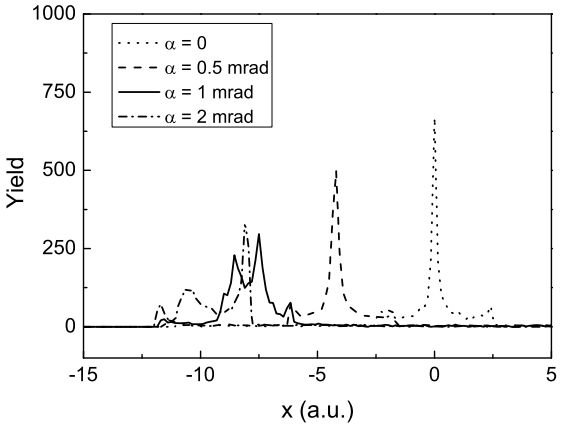

Fig. 3 – The spatial distributions along the x axis of protons channeled in the (10,10) SWBNNTs with 4 different nanotube bent angles α = 0, 0.5, 1.0 and 2 mrad. The proton energy is E = 10 MeV and the nanotube length is L = 1 μm.

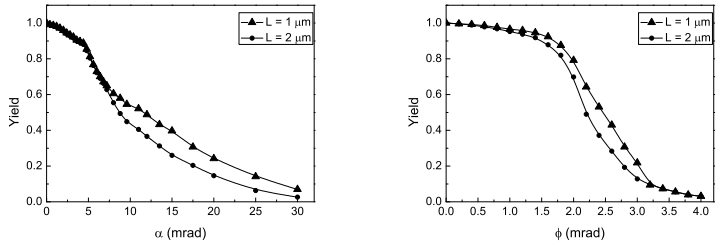

Fig. 4 – (left) The normalized yield of 10 MeV protons transmitted through the (10,10) SWBNNTs of the lengths L = 1 and 2 μm. Nanotube bent angle α is varied between 0 and 30 mrad. (right) The normalized yield of 10 MeV protons transmitted through the (10,10) SWBNNTs of the lengths L = 1 and 2 μm. Proton incident angle φ is varied between 0 and 4 mrad.

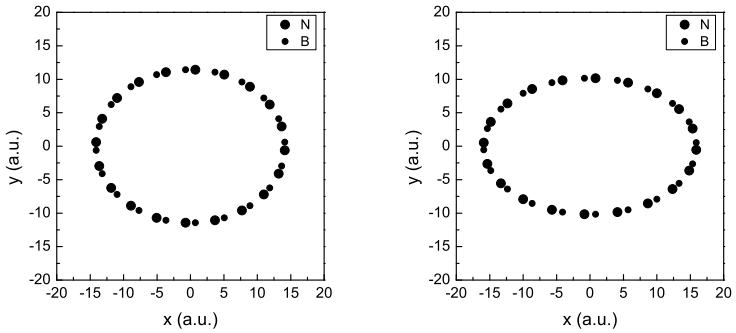

Fig. 5 – The view along axes of short (10,10) SWBNNTs under different radial strains: (left) η = 0.1 and (right) η = 0.2.

effects. Figure 4 (left) shows the normalized yield of 10 MeV protons transmitted through the (10,10) SWBNNTs of the lengths L = 1 and 2 μm. Nanotube bent angle α is varied between 0 and 4 mrad. Figure 4 (right) shows the normalized yield of 10 MeV protons transmitted through the (10,10) SWBNNTs of the lengths L = 1 and 2 μm. Proton incident angle φ is varied between 0 and 4 mrad. We can see that for α = 8 mrad and for φ = 2.5 mrad only about 50% of initial yield of protons remains, and for α = 30 mrad and φ = 4 mrad all protons are dechanneled, respectively. We can see that effect of bending for the same angle ($\alpha = \varphi$) has less influence on dechanneling compared to the donut effect in transmission yield of protons. With increase the length of nanotubes two times, dechanneling of protons is little stronger for both effects (bending and donut effect). In order to save higher percent of the flux of the initial proton beam during the proton guiding by nanotube we have to choose not too big incidence and bending angles.

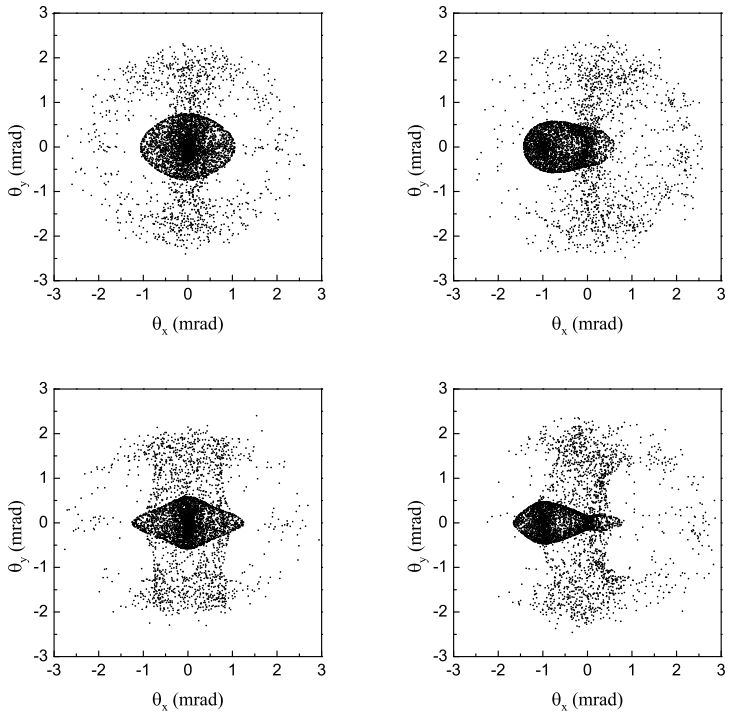

Fig. 6 – The angular distributions of protons channeled in the (10,10) SWBNNTs in the $\Theta_x\Theta_y$ plane. The proton energy is E = 10 MeV and the nanotube length is L = 1 μm. The nanotube bent angle and radial strain are: (left up) $(\alpha = 0, \eta = 0.1)$, (right up) $(\alpha = 1.0$ mrad, $\eta = 0.1)$, (left down) $(\alpha = 0, \eta = 0.2)$ and (right down) $(\alpha = 1.0$ mrad, $\eta = 0.2)$.

In Fig. 5 we presented the view along axes of short straight (10,10) SWBNNTs under different radial strains: (left) η = 0.1 and (right) η = 0.2.

As can be stated, the cross section of the radially deformed nanotubes have elliptical shape. We consider the influence of the nanotube bending angle and radial strain on the angular and spatial distributions in Figs. 6 and 7. Figure 6 shows the angular distributions of protons channeled in the (10,10) SWBNNTs in the $\Theta_x\Theta_y$ plane for different values of nanotube bent angle and radial strain. Figure 7 shows the same, but for spatial distributions in the xy plane. We can see that the presence of both effect influences strongly on angular and spatial distributions. The bending of nanotube dominantly influences on moving the maximum yield within nanotube and radial strain dominantly influences that shape of angular and spatial distributions become more elliptical. Both effect should be taken into account when realistic calculation of proton guiding with nanotube is performed.

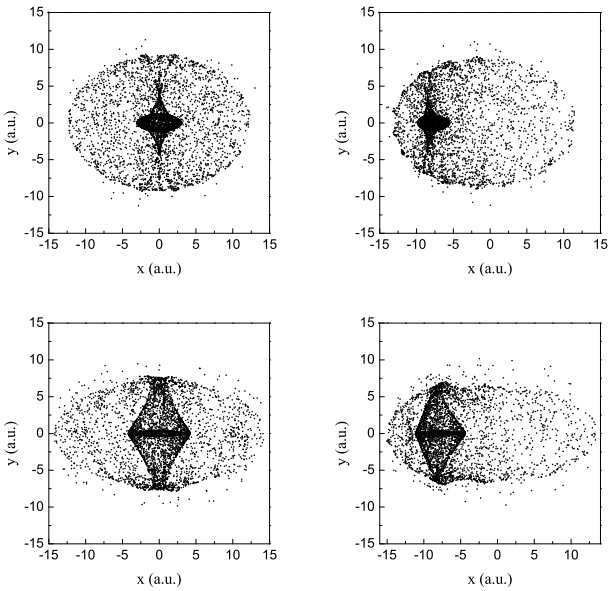

Fig. 7 – The same like Fig. 6, but for spatial distributions.

4. CONCLUSIONS

We have analyzed here the dependence of the angular and spatial distributions of 10 MeV protons channeled in a bent 1 and 2 μm (10,10) SWBNNTs on the bending angle, in the range of 0 to 4 mrad and under the radial deformation strains 0, 0.1 and 0.2. The analysis has been done using the Molière's expression for the continuum potential of the SWBNNT's atoms and Monte Carlo simulation method. We show that the angular and spatial distributions depend strongly on bending angle and on the radial strain of nanotube. Also, effect of bending is comparable to the effect of the radial deformation. Because both effect are very realistic, *i.e.* almost all of nanotubes are naturaly curved and majority of them are radially deformed, these two effect should be taken into account simultaneously. Dominant influence of bending of nanotube is moving the maximum yield within nanotube and dechanneling process. If we want to save higher flux of initial proton beam during the proton channeling through nanotube we have to choose not too big bending angle. Dominant influence of radial strain effect is that shape of angular and spatial distributions become more elliptical.

We believe that the results exposed in the present paper may be very useful for BN nanotube characterization, production and guiding of nanosized ion beams. We showed in this and in previous paper [1] that SWBNNTs have very similar guiding

properties like CNTs, in case of guiding of high energy protons, because they have very similar structure. Advantage of BN nanotubes are that they are more thermal and chemical stable, thats why they might present even better candidates for future channeling experiments.

Acknowledgements. This work was supported by the Ministry of Education, Science and Technological Development of the Republic of Serbia through the projects 45005 and 171016. Authors would also like to thank Dr. V. Borka Jovanović for many useful discussions.

REFERENCES

1. V. Borka Jovanović, D. Borka, Nucl. Instrum. Methods Phys. Res. B **354**, 60 (2015).
2. V. Borka Jovanović, D. Borka, S. M. D. Galijaš, Phys. Lett. A **381**, 1687 (2017).
3. S. Iijima, Nature **354**, 56 (1991).
4. A. Rubio, J. L. Corkill, M. L. Cohen, Phys. Rev. B **49**, 5081 (1994).
5. N. G. Chopra, R. J. Luyken, K. Cherrey, V. H. Crespi, M. L. Cohen, S. G. Louie, A. Zettl, Science **269**, 966 (1995).
6. M. Terrones, W. K. Hsu, H. Terrones, J. P. Zhang, S. Ramos, J. P. Hare, R. Castillo, K. Prassides, A. K. Cheetham, H. W. Kroto, D. R. M. Walton, Chem. Phys. Lett. **259**, 568 (1996).
7. A. Loiseau, F. Willaime, N. Demoncy, G. Hug, H. Pascard, Phys. Rev. Lett. **76**, 4737 (1996).
8. I. Narita, T. Oku, Solid State Commun. **122**, 465 (2002).
9. D. Özmen, N. A. Sezgi, S. Balci, Chem. Eng. J. **219**, 28 (2013).
10. W. Q. Han, Y. Bando, K. Kurashima, T. Sato, Appl. Phys. Lett. **73**, 3085 (1998).
11. W. -Q. Han, J. Cumings, X. Huang, K. Bradley, A. Zettl, Chem. Phys. Lett. **346**, 368 (2001).
12. Y. Chen, M. Conway, J. S. Williams, J. Zou, J. Mater. Res. **17**, 1896 (2002).
13. Y. Chen, J. Zou, S. J. Campbell, G. L. Caer, Appl. Phys. Lett. **84**, 2430 (2004).
14. L. Li, L. H. Li, Y. Chen, X. J. Dai, T. Xing, M. Petrović, X. Lin, Nanoscale Res. Lett. **7**, 417 (2012).
15. D. P. Yu, X. S. Sun, C. S. Lee, I. Bello, S. T. Lee, H. D. Gu, K. M. Leung, G. W. Zhu, Z. F. Dong, Z. Zhang, Appl. Phys. Lett. **72**, 1966 (1988).
16. M. W. Smith, K. C. Jordan, C. Park, J. -W. Kim, P. T. Lillehei, R. Crooks, J. S. Harrison, Nanotechnology **20**, 505604 (2009).
17. L. Hou, F. Gao, G. Sun, H. Gou, M. Tian, Cryst. Growth Des. **7**, 535 (2007).
18. N. G. Chopra, A. Zettl, Solid State Commun. **105**, 297 (1998).
19. E. Hernandez, C. Goze, P. Bernier, A. Rubio, Phys. Rev. Lett. **80**, 4502 (1998).
20. D. Sanchez-Portal, E. Hernandez, Phys. Rev. B. **66**, 235415 (2002).
21. Y. Xiao, X. H. Yan, J. X. Cao, J. W. Ding, Y. L. Mao, J. Xiang, Phys. Rev. B **69**, 205415 (2004).
22. C. Y. Zhi, Y. Bando, C. C. Tang, R. G. Xie, T. Sekiguchi, D. Golberg, J. Am. Chem. Soc. **127**, 15996 (2005).
23. D. Golberg, Y. Bando, C. C. Tang, C. Y. Zhi, Adv. Mater. **19**, 2413 (2007).
24. V. M. Biryukov, S. Bellucci, Phys. Lett. B **542**, 111 (2002).
25. C. S. Moura, L. Amand, Carbon **45**, 185 (2007).
26. S. I. Matyukhin, K. Y. Fralenkov, Tech. Phys. Lett. **33**, 58 (2007).
27. S. I. Matyukhin, Tech. Phys. Lett. **35**, 318 (2009).
28. Y. Li, L. P. Zheng, W. Zheng, Z. J. Xu, C. L. Ren, P. Huai, Z. Y. Zhu, Chin. Phys. Lett. **28**, 066101

(2011).
29. D. Borka, S. Petrović, N. Nešković, *"Channeling of Protons Through Carbon Nanotubes"*, Nova Science Publishers, New York, 2011, 1.
30. S. W. Cui, R. Z. Zhu, X. S. Wang, H. X. Yang, Chin. Phys. B **23**, 106105 (2014).
31. Z. Zhu, D. Zhu, R. Lu, Z. Xu, W. Zhang, H. Xia, *"Proceedings of the International Conference on Charged and Neutral Particles Channeling Phenomena"*, (SPIE, Bellingham, Washington), **5974**, 13 (2005).
32. G. Choi, H. Heinrich, L. Chow, T. Schenkel, Appl. Phys. Lett. **91**, 103101 (2007).
33. V. V. Klimov and V. S. Letokhov 1996 Phys. Lett. A **222**, 424 (1996)
34. G. V. Dedkov, Nucl. Instrum. Meth. Phys. Res. B **143**, 584 (1998).
35. N. K. Zhevago and V. I. Glebov, Phys. Lett. A **250**, 360 (1998).
36. L. A. Gevorgian, K. A. Ispirian and R. K. Ispirian, Nucl. Instrum. Meth. Phys. Res. B **145**, 155 (1998).
37. A. A. Greenenko and N. F. Shulga, Nucl. Instr. Meth. Phys. Res. B **205**, 767 (2003).
38. X. Artru, S. P. Fomin, N. F. Shulga, K. A. Ispirian and N. K. Zhevago, Phys. Rep. **412**, 89 (2005).
39. A. V. Krasheninnikov, K. Nordlund, Phys. Rev. B **71**, 245408 (2005).
40. S. Petrović, D. Borka, N. Nešković, Nucl. Instrum. Methods Phys. Res. B **234**, 78 (2005).
41. D. Borka, S. Petrović, N. Nešković, D. J. Mowbray and Z. L. Mišković, Phys. Rev. A **73**, 062902 (2006).
42. D. Borka, D. J. Mowbray, Z. L. Mišković, S. Petrović and N. Nešković, Phys. Rev. A **77**, 032903 (2008).
43. D. Borka, D. J. Mowbray, Z. L. Mišković, S. Petrović and N. Nešković, New J. Phys. **12**, 043021 (2010).
44. D. Borka, V. Lukić, J. Timko, V. Borka Jovanović, Nucl. Instrum. Meth. Phys. Res. B **279**, 169 (2012).
45. D. Borka, V. Lukić, J. Timko, V. Borka Jovanović, Nucl. Instrum. Meth. Phys. Res. B **279** , 198 (2012).
46. V. A. Aleksandrov and G. M. Filippov, Journal of Surface Investigation. X-ray, Synchrotron and Neutron Techniques **6**, 338 (2012).
47. Y.-Y. Zhang, J.-Z. Sun, Y.-H. Song, Z. L. Mišković and Y.-N. Wang, Carbon **71**, 196 (2014).
48. A. Karabarbounis, S. Sarros and Ch. Trikalinos, Nucl. Instrum. Meth. Phys. Res. B **355**, 316 (2015).
49. M. Ćosić, S. Petrović and N. Nešković, Nucl. Instrum. Meth. Phys. Res. B **373**, 52 (2016).
50. D. S. Gemmell, Rev. Mod. Phys. **46**, 129 (1974).
51. K. Schiessl *et al.*, Phys. Rev. A **72**, 062902 (2005).
52. M. Menon and D. Srivastava, Chem. Phys. Lett. **307**, 407 (1999).
53. G. Kim, J. Park, and S. Hong, Chem. Phys. Lett. **522**, 79 (2012).
54. M. K. Abu-Assy, M. S. Soliman, Nucl. Instrum. Methods Phys. Res. B **384**, 93 (2016).
55. G. Z. Moliére, Naturforsch. A **2**, 133 (1947).
56. L. Karbunar, D. Borka, I. Radović, Z. L. Mišković, Chin. Phys. B **25**, 046106 (2016).